

Decay dynamics in a strongly driven atom-molecule coupled system

Arpita Rakshit¹, Saikat Ghosh² and Bimalendu Deb^{1,3}

¹ Department of Materials Science, ³Raman Center for Atomic, Molecular and Optical Sciences, Indian Association for the Cultivation of Science, Jadavpur, Kolkata 700032, India.

² Department of Physics, Indian Institute of Technology, Kanpur, India

Abstract. Within the framework of master equation, we study decay dynamics of an atom-molecule system strongly coupled by two photoassociation lasers. Summing over the infinite number of electromagnetic vacuum modes that are coupled to the system, we obtain an integro-differential master equation for the system's reduced density matrix. We use this equation to describe correlated spontaneous emission from a pair of electronically excited diatomic ro-vibrational states. The temporal evolution of emitted radiation intensity shows quantum beats that result from the laser-induced coherence between the two excited states. The phase difference between the two driving fields is found to significantly affect the decay dynamics and the beats. Our results demonstrate the possibility to control decay and decoherence in the system by tuning the relative intensity and the phase between the two lasers. We further show that, if the ground-state continuum has a shape resonance at a low energy, then the quantum beats show two distinctive time scales of oscillations in the strong coupling regime. One of the time scales originates from the energy gap between the two excited states while the other time scale corresponds to the collision energy at which free-bound Franck-Condon overlap is resonantly peaked due to the shape resonance.

PACS numbers: 32.80Qk, 34.80Pa, 34.50cx, 42.50Md

1. Introduction

Over the last two decades there has been tremendous developments in high precision spectroscopy with cold atoms. It is now possible to access low lying rotational levels of a diatomic molecule formed by photoassociation (PA) in cold atoms. For an excited long-ranged molecule (formed via narrow-line inter-combination photoassociative transitions as in cold bosonic Sr or Yb atoms) the lifetime of excited rotational levels can be as large as 10 microseconds. Such metastable molecular excited states are now experimentally accessible using optical spectroscopic techniques. This opens up the possibility of creating and studying quantum superposition states between molecular rotational states as well as superpositions between molecular states and collisional continuum of scattering states between ground-state atoms. In a PA process, the scattering state between two ground-state cold atoms become optically coupled to an excited diatomic bound (molecular) state. In the weak photoassociative coupling regime, it is interpreted as a loss process and PA spectra are detected in terms of the loss of atoms due to spontaneous emission from the excited bound state. However, in the strong-coupling regime, the continuum of the scattering states between two atoms becomes strongly-coupled leading to atom-molecule or continuum-bound dressed state quantum dynamics. A transition from the state of two colliding atoms to a diatomic bound state is generally referred to as free-bound transition. To develop a proper understanding of correlated quantum dynamics of an atom-molecule coupled system, it is important to formulate a density matrix formalism in continuum-bound dressed state picture to appropriately account for spontaneous emission and decoherence in the dynamics. The influence of spontaneous emission on a continuum-bound coupled system had been earlier discussed [1, 2, 3] in the context of autoionizing states. Early work by Agarwal *et al.* [1] treated spontaneous emission of continuum-bound coupled autoionising Fano state [4] within the master equation framework. We adapt such an approach to develop a master equation for the atom-molecule coupled system at ultracold temperatures. Unlike most of the the standard systems in quantum optics dealing with dissipation and decoherence from discrete levels, the master equation approach in the present context is rather involved due to the continuum of states of collision between ground-state atoms.

Here we develop a model to describe coherent effects in an atom-molecule system and demonstrate that, after having created coherent superposition between two rotational states by strongly driving two photoassociative transitions with two lasers, the superposition can be detected as rotational quantum beats in fluorescence light emitted from the correlated rotational levels. Considering ^{174}Yb as a prototype system, we first analyze the ideal situation of the dressed continuum among two excited rotational states and the bare continuum of scattering between ground-state Yb atoms in the absence of spontaneous emission. This provides understanding of how the relative intensities and the phases between the two driving PA lasers can be used as knobs to manipulate coherence between the two excited states. We then discuss the effects of spontaneous emission and decoherence on the dynamical properties of the dressed states. Our results show that by judiciously adjusting relative intensity and the phase between the two lasers it is possible to inhibit spontaneous emission from the two

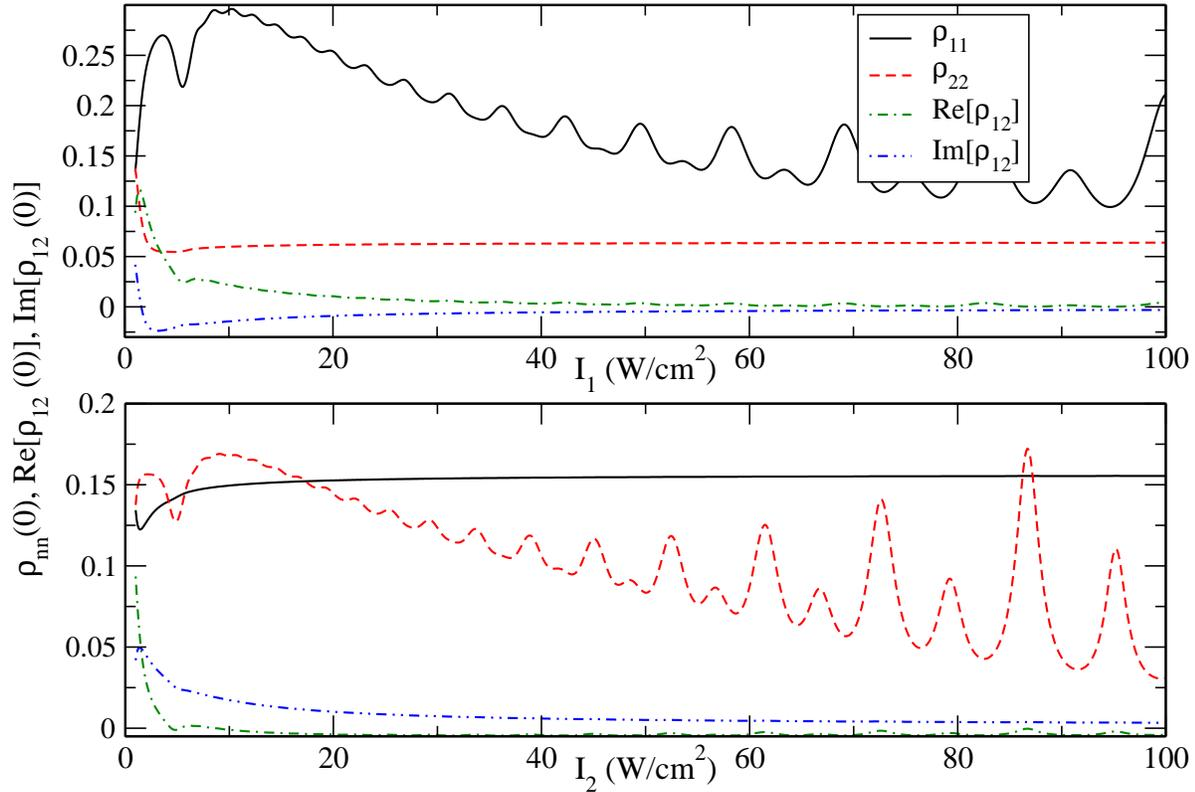


Figure 1. (Color online) $\rho_{nn}(0)$ ($n = 1, 2$) and the real and imaginary parts of $\rho_{12}(0)$ are plotted against I_1 (upper panel) and I_2 (lower panel) in unit of W cm^{-2} , keeping the intensity of the other laser fixed at 1 W cm^{-2} . The other parameters are $\phi = 0$ and $\delta_1 = \delta_2 = 0$.

correlated excited molecular states and to preserve or manipulate the coherence between the states.

Quantum beats in radiation intensity arise from coherent superposition of two long-lived excited states. Such state superpositions and their manipulations are of considerable recent interest in quantum information science. The possibility of using quantum beats as a spectroscopic measure for quantum superposition was discussed as early as in 1933 [5]. Experimentally, spectroscopic study of quantum beats started since 1960s [6]. The use of lasers to create quantum superposition and detect resulting quantum beats in fluorescence started in early 1970s [7]. Forty years ago, Haroche, Paisner and Schawlow [8] demonstrated quantum beats in fluorescence light emitted from the excited hyperfine levels of a Cs atom as a signature of quantum superposition between the excited atomic states. Since then quantum beats in fluorescence spectroscopy have been studied in a variety of physical situations [9, 10]. These techniques open up new possibilities for studying excited state properties, state preparation and manipulation as well as collisional and spectroscopic aspects of ultra-cold atoms and molecules.

The paper is organized as follows: In section 2, the model is presented and discussed. We develop a master equation approach to spontaneous emission in continuum-bound atom-molecule coupled system in section 3. A solution for the master equation is presented.

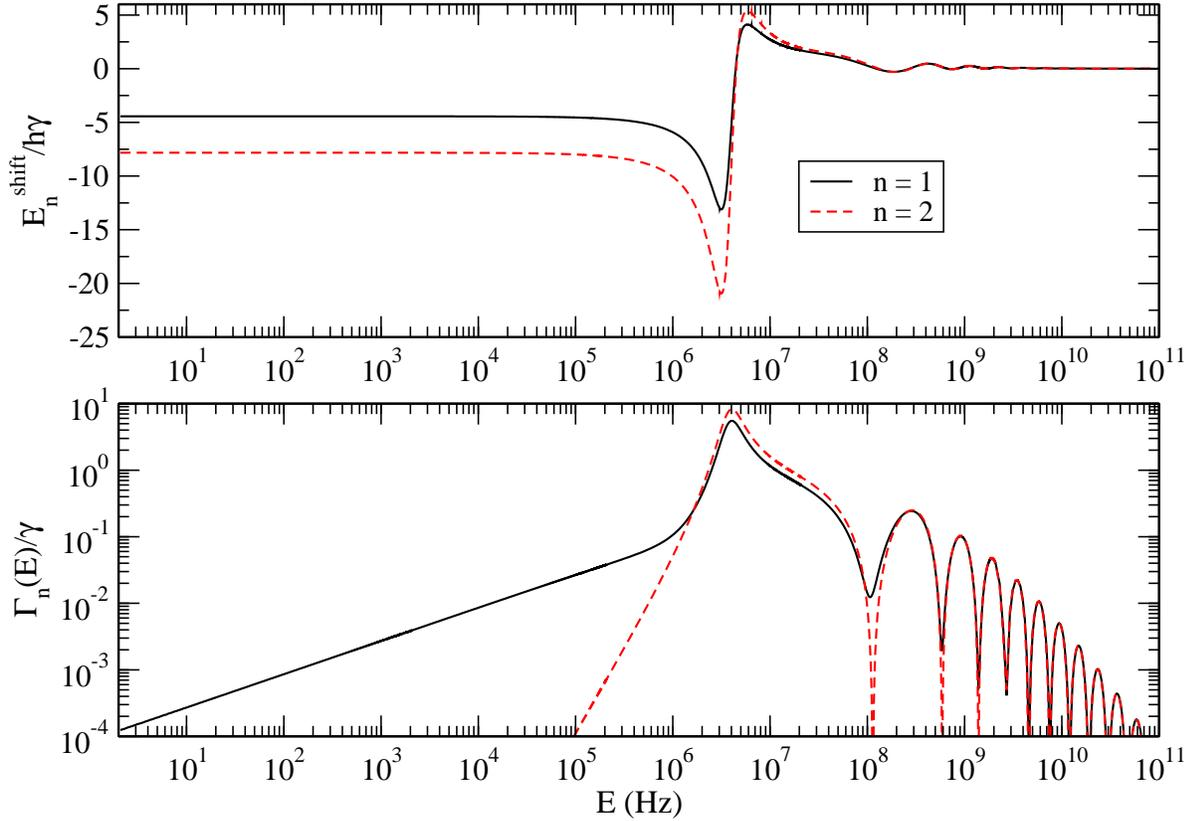


Figure 2. (Color online) Light shifts (scaled by $h\gamma$) and free-bound stimulated line widths (scaled by γ) of the two excited bound states $n = 1$ ($J = 1$) (solid) and $n = 2$ ($J = 3$) (dashed) - both having the same vibrational quantum number $v = 106$ of $^{174}\text{Yb}_2$ (see text) are plotted as a function of collision energy E (in Hz) in upper and lower panels, respectively; for $I_1 = I_2 = 1 \text{ W cm}^{-2}$ and the detunings $\delta_1 = \delta_2 = 0$.

Numerical results are analyzed in section 4. The paper is concluded in section 5.

2. The model

Our model consists of two excited diatomic molecular ro-vibrational states $|b_1\rangle$ and $|b_2\rangle$ (belonging to the same molecular electronic state) coupled to the ground-state bare continuum $|E\rangle_{\text{br}}$ of scattering states, by the lasers 1 and 2, respectively. Initially either $|b_1\rangle$ or $|b_2\rangle$ or partially both are populated due to two photoassociation lasers L_1 and L_2 of frequencies ω_{L1} and ω_{L2} , tuned near $|E\rangle_{\text{br}} \rightarrow |b_1\rangle$ and $|E\rangle_{\text{br}} \rightarrow |b_2\rangle$ transitions, respectively. The ground continuum is assumed to have only one internal molecular state with only one threshold and no hyperfine interaction. We assume that the two free-bound PA transitions between the ground-state continuum and the two excited ro-vibrational states are strongly driven so that the spontaneous emissions from these two bound states to the continuum are negligible as compared to the corresponding stimulated ones. However, these two driven bound states can spontaneously decay to other bound states in the ground electronic configuration. The model we describe in this paper may be contrasted with that in [13] where two excited ro-vibrational

states populated by photoassociation from ground-state continuum are assumed to decay to the same continuum only. In the present paper, we primarily discuss the creation of laser-induced coherence and its implications in decay dynamics within the framework of master equation approach while the earlier work [13] concerns the creation of vacuum-induced coherence (VIC) with a more simplified model that is solvable by Wigner-Weisskopf method. Compared to the model used in [13], the present model is more realistic as it considers decay of the system outside the dressed continuum. Moreover, the present work shows exciting possibilities of manipulating excited state coherences using the relative phase between two lasers.

The Hamiltonian governing the dynamics of this system can be written as $H = H_S + H_{SR}$, where $H_S = H_{\text{coh}} + \hbar\omega_{b_0} |b_0\rangle\langle b_0|$ is the system Hamiltonian with two parts: the first part H_{coh} describes coherent dynamics with the two strong PA couplings. On the other hand, the second part H_{SR} is the interaction part of the system with a reservoir of vacuum electromagnetic modes. Explicitly, one can write

$$H_{\text{coh}} = \sum_{n=1}^2 \hbar(\omega_{b_n} - \omega_{L_n}) |b_n\rangle\langle b_n| + \int E' |E'\rangle_{\text{br}} \langle E'| dE' \\ + \int \sum_{n=1}^2 \left\{ \Lambda_{nE'} \hat{S}_{nE'}^\dagger + \text{H.C.} \right\} dE' \quad (1)$$

$$H_{SR} = \sum_{n=1,2} \sum_{\kappa,\sigma} \hat{a}_{\kappa,\sigma} e^{-i(\omega_\kappa + \omega_{L_n})t} V_{n0}(\kappa\sigma) |b_n\rangle\langle b_0| + \text{H.c.} \quad (2)$$

where H_{SR} is the Hamiltonian describing the interaction of the system with the reservoir of vacuum modes. Here $\hbar\omega_{b_n}$ are the binding energies of the bound states $|b_n\rangle$ ($n=1, 2$); $|E'\rangle_{\text{br}}$ is the bare continuum state. In deriving the above Hamiltonian, we have used rotating wave approximation (RWA) [14]. In RWA, one works in a frame rotating with the frequency of the sinusoidally oscillating field interacting with a two-level system (TLS) and neglects the counter-rotating terms that oscillate with the sum of the field and the system frequencies. It primarily relies on two conditions: (i) the system relaxation time is much larger than the time period of oscillation of the field and (ii) Rabi frequency or the system-field coupling is much smaller than the transition frequency of TLS. These conditions are in general fulfilled in most cases of a TLS interacting with a monochromatic optical field and therefore RWA can be regarded as a cornerstone for studying quantum dynamics of TLS. Nevertheless, RWA may break down in case of intense laser fields or short pulses when the Rabi frequency or the coupling becomes comparable with the system frequency. Generally, this may happen when the laser intensity is of the order of $10^{12} \text{ W cm}^{-2}$ or higher. In PA experiments the laser intensity is much lower, typically in the W cm^{-2} or kW cm^{-2} . Strong-coupling regime in ultracold PA can be reached with laser intensities higher than 1 kW cm^{-2} but much lower than 1 MW cm^{-2} . For driven TLS, corrections beyond RWA and in terms of Bloch-Siegert shift [15] have been discussed by Grifoni and Hanggi [16]. The corrections to RWA can be formulated as a systematic expansion in terms of the ratio of Rabi frequency to the field frequency [17]. In case of two coupled TLS, there exists a parameter regime where leading

order term in the expansion vanishes rendering the next higher order term to be significant [17]. However, such situation does not arise in our case and so RWA remains valid.

With electric dipole approximation, the laser coupling $\Lambda_{nE'}$ for the absorptive transition from the bare continuum $|E'\rangle_{\text{br}}$ to the n th excited bound state $|b_n\rangle$ is given by

$$\Lambda_{nE'} = e^{i(\mathbf{k}_{L_n} \cdot \mathbf{R} + \phi_{L_n})} \langle b_n | \vec{D}_n \cdot \mathbf{E}_{L_n} | E'\rangle_{\text{br}} \quad (3)$$

where \mathbf{k}_{L_n} , \mathbf{E}_{L_n} and ϕ_{L_n} are the wave vector, electric field and phase of the n th laser, respectively; \mathbf{R} is the center-of-mass position vector of the two atoms and \vec{D}_n is the free-bound molecular dipole moment associated with the n th bound state. The electric dipole approximation here dictates that $k_{L_n} r \ll 1$, where r is the separation between the two atoms. We have thus used $\exp(i\mathbf{k}_{L_n} \cdot \mathbf{r}) \simeq 1$ in writing the above equation. The operator $\hat{S}_{nE'}^\dagger = |b_n\rangle_{\text{br}} \langle E'|$ is a raising operator, $\hat{a}_{\kappa,\sigma}$ denotes the annihilation operator of the vacuum field \vec{E}_{vac} and $V_{n0}(\kappa\sigma) = -\langle b_n | \vec{D}_{n0} \cdot \vec{E}_{vac}(\kappa) | b_0 \rangle$ is the dipole coupling with $\vec{E}_{vac}(\kappa) = \left(\sqrt{\hbar\omega_\kappa/2\epsilon_0 V} \right) \vec{e}_\sigma$, ω_κ being the wave number, \vec{D}_{n0} the transition dipole moment between n th excited bound state and the ground bound state $|b_0\rangle$, σ the polarization of the field and $\sqrt{\hbar\omega_\kappa/2\epsilon_0 V}$ the amplitude of the vacuum field and $\hbar\omega_{b_0}$ is the binding energy of the bound state $|b_0\rangle$. The Hamiltonian \mathcal{H}_{coh} is exactly diagonalizable [13, 18] in the spirit of Fano's theory [4]. The eigenstate of \mathcal{H}_S is a dressed continuum expressed as

$$|E\rangle_{\text{dr}} = \sum_{n=1}^2 A_{nE} |b_n\rangle + \int C_{E'}(E) |E'\rangle_{\text{br}} dE' \quad (4)$$

with the normalization condition ${}_{\text{dr}}\langle E'' | E \rangle_{\text{dr}} = \delta(E - E'')$. The coefficients A_{nE} and $C_{E'}(E)$ are derived in Ref [18].

By using partial-wave decomposition of the bare continuum $|E'\rangle_{\text{br}} = \sum_{\ell m_\ell} |E' \ell m_\ell\rangle_{\text{br}}$, we have $\Lambda_{nE'} = \exp[i(\mathbf{k}_{L_n} \cdot \mathbf{R} + \phi_{L_n})] \sum_{\ell m_\ell} \Lambda_{J_n M_n}^{\ell m_\ell}(E')$ where J_n and M_n are the rotational and the magnetic quantum number, respectively, of the n th excited bound state in the space-fixed (laboratory) coordinate system. Note that $\Lambda_{J_n M_n}^{\ell m_\ell}(E)$ represents amplitude for free-bound transition from (ℓm_ℓ) incident partial-wave state to the n th bound state. To denote the amplitude for reverse (bound-free) transition, we use the symbol $\Lambda_{\ell m_\ell}^{J_n M_n}(E)$. Accordingly, we can write $A_{nE} = \sum_{\ell' m_{\ell'}} A_{nE}^{\ell' m_{\ell'}} Y_{\ell', m_{\ell'}}(\hat{k})$ and $C_{E'}(E) = \sum_{\ell m_\ell} \sum_{\ell' m_{\ell'}} C_{E', \ell m_\ell}^{\ell' m_{\ell'}}(E) Y_{\ell', m_{\ell'}}(\hat{k})$ where \hat{k} represents a unit vector along the incident relative momentum between the two atoms. Explicitly,

$$A_{nE}^{\ell' m_{\ell'}} = \frac{e^{i\theta_n} \Lambda_{J_n M_n}^{\ell' m_{\ell'}}(E) + \xi_n^{-1} \mathcal{K}_{nn'}^{\text{LL}} e^{i\theta_{n'}} \Lambda_{J_{n'} M_{n'}}^{\ell' m_{\ell'}}(E)}{\xi_n - \xi_n^{-1} \mathcal{K}_{nn'}^{\text{LL}} \mathcal{K}_{n'n}^{\text{LL}}}, \quad n' \neq n \quad (5)$$

$$C_{E', \ell m_\ell}^{\ell' m_{\ell'}}(E) = \delta_{\ell' \ell} \delta_{m_{\ell'} m_\ell} \delta(E - E') + \sum_{n=1,2} \frac{A_{nE}^{\ell' m_{\ell'}} \Lambda_{\ell m_\ell}^{J_n M_n}(E')}{E - E'} \quad (6)$$

where $\theta_n = \mathbf{k}_{L_n} \cdot \mathbf{R} + \phi_{L_n}$,

$$\xi_n(E) = \hbar(\delta_{nE} + i\Gamma_n(E)/2) \quad (7)$$

$$\hbar\delta_{nE} = E + \hbar\delta_{L_n} - (E_n + E_n^{\text{shift}}) \quad (8)$$

with E_n being the binding energy of n th excited bound state measured from the threshold of the excited state potential, E_n^{shift} is the light shift of the n^{th} bound state and $\delta_{L_n} = \omega_{L_n} - \omega_A$ with ω_{L_n} is the laser frequency of n -th laser and ω_A the atomic transition frequency. The two lasers interacting with the system results in an effective coupling

$$\mathcal{K}_{nn'}^{\text{LL}} = \left(\mathcal{V}_{nn'} - i\frac{1}{2}\hbar\mathcal{G}_{nn'} \right) \quad (9)$$

between the two bound states where

$$\mathcal{V}_{nn'} = \exp[i(\theta_n - \theta_{n'})] \sum_{\ell m_\ell} \mathcal{P} \int dE' \frac{\Lambda_{\ell m_\ell}^{J_n M_n}(E') \Lambda_{J_{n'} M_{n'}}^{\ell m_\ell}(E')}{E - E'}, \quad (10)$$

$$\mathcal{G}_{nn'} = \exp[i(\theta_n - \theta_{n'})] \frac{2\pi}{\hbar} \sum_{\ell m_\ell} \Lambda_{\ell m_\ell}^{J_n M_n}(E) \Lambda_{J_{n'} M_{n'}}^{\ell m_\ell}(E). \quad (11)$$

The term $\Gamma_n(E) = 2\pi |\Lambda_{nE}|^2 / \hbar = 2\pi \sum_{\ell, m_\ell} |\Lambda_{\ell m_\ell}^{J_n M_n}(E)|^2 / \hbar$, is the stimulated linewidth of the n -th bound state due to continuum-bound laser coupling. Note that the light shift $E_n^{\text{shift}} = \sum_{\ell} E_{n\ell}^{\text{shift}}$ is the sum over all the partial light shifts

$$E_{n\ell}^{\text{shift}} = \sum_{m_\ell} \mathcal{P} \int dE' \frac{\Lambda_{\ell m_\ell}^{J_n M_n}(E') \Lambda_{J_n M_n}^{\ell m_\ell}(E')}{E - E'}. \quad (12)$$

3. Master equation

The system Hamiltonian can be written in dressed basis as

$$H_0 = \int E dE |E\rangle_{\text{dr}} \langle E| + \hbar\omega_{b_0} |b_0\rangle \langle b_0| \quad (13)$$

To derive master equation we work in the dressed continuum basis of the system Hamiltonian. We express bare basis in terms of dressed basis as follows

$$|b_n\rangle = \int dE |E\rangle_{\text{dr}} \langle E| b_n\rangle = \int dE A_{nE}^* |E\rangle_{\text{dr}} \quad (14)$$

$$\begin{aligned} |E'\rangle_{\text{br}} &= \int dE |E\rangle_{\text{dr}} \langle E| E'\rangle \\ &= \int dE C_{E'}^*(E) |E\rangle_{\text{dr}} \end{aligned} \quad (15)$$

By substituting all bare basis states with there expansions in terms of dressed basis, we can write system-reservoir interaction Hamiltonian in terms of dressed basis. In the interaction picture, the effective system-reservoir interaction Hamiltonian $H_{SR}^I = e^{iH_0 t/\hbar} H_{SR} e^{-iH_0 t/\hbar}$ of the driven system interacting with a reservoir of vacuum modes can be written as

$$H_{SR}^I = \sum_{\kappa, \sigma} e^{-i\omega_\kappa t} \sum_{n=1}^2 e^{i(\omega_{b_0} - \omega_{L_n})t} \hat{a}_{\kappa, \sigma} \int dE A_{nE}^* V_{n0}(\kappa\sigma) e^{i\omega_E t} \hat{S}_{0E}^\dagger + \text{H.c} \quad (16)$$

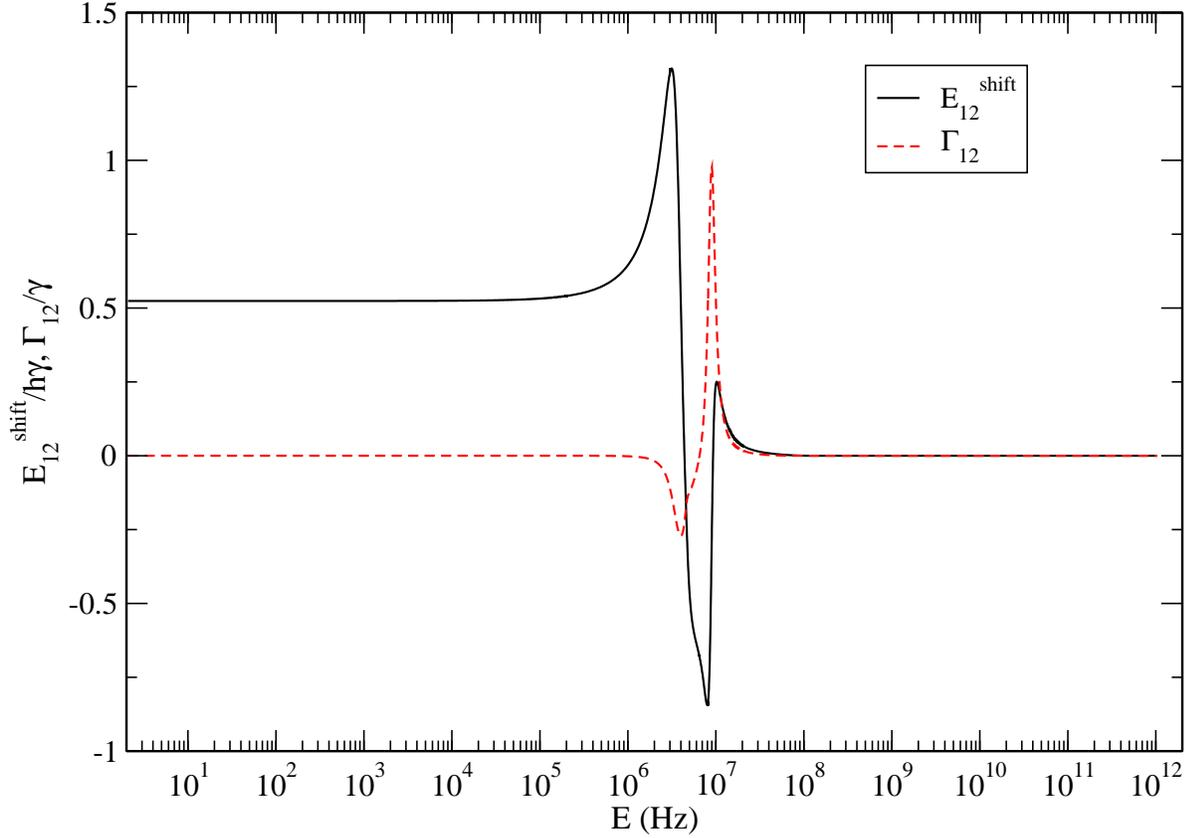


Figure 3. (Color online) Plotted are E_{12}^{shift} in unit of $h\gamma$ (black solid) and Γ_{12} in unit of $h\gamma$ (red dashed) are plotted as a function of collision energy E (in Hz). Other parameters are as same as in figure 2.

where the superscript ‘ I ’ refers to interaction picture, $\hat{S}_{0E} = |b_0\rangle_{\text{dr}}\langle E|$ and $\omega_{n0} = \omega_{b_n} - \omega_{b_0}$

Let $\rho_{S+R}(t)$ denote the system-reservoir joint density matrix. Following Agarwal [19], the projection operator P is defined by

$$\mathcal{P}\rho_{S+R}(t) = \rho_R(0)\rho_S(t) \quad (17)$$

wher ρ_R and ρ_S are the density matrices of vacuum and the dressed system (S) system, respectively. With the use of this projection operator, Liouville equation under Born approximation can be expressed [19] as

$$\frac{\partial}{\partial t} \{P\rho_{S+R}^I(t)\} = - \int_0^t d\tau PL_S^I(t)L_S^I(t-\tau)P\rho_{S+R}^I(t-\tau) \quad (18)$$

where

$$\rho^I = e^{iH_0t/\hbar} \rho e^{-iH_0t/\hbar} \quad (19)$$

is the density matrix in the interaction picture. Here

$$L_S^I(t) \cdots = \sum_{\kappa,\sigma} e^{-i\omega_{\kappa}t} \left[\hat{a}_{\kappa\sigma} \hat{\Sigma}_{\kappa\sigma}^+(t), \cdots \right] + \text{H.c.} \quad (20)$$

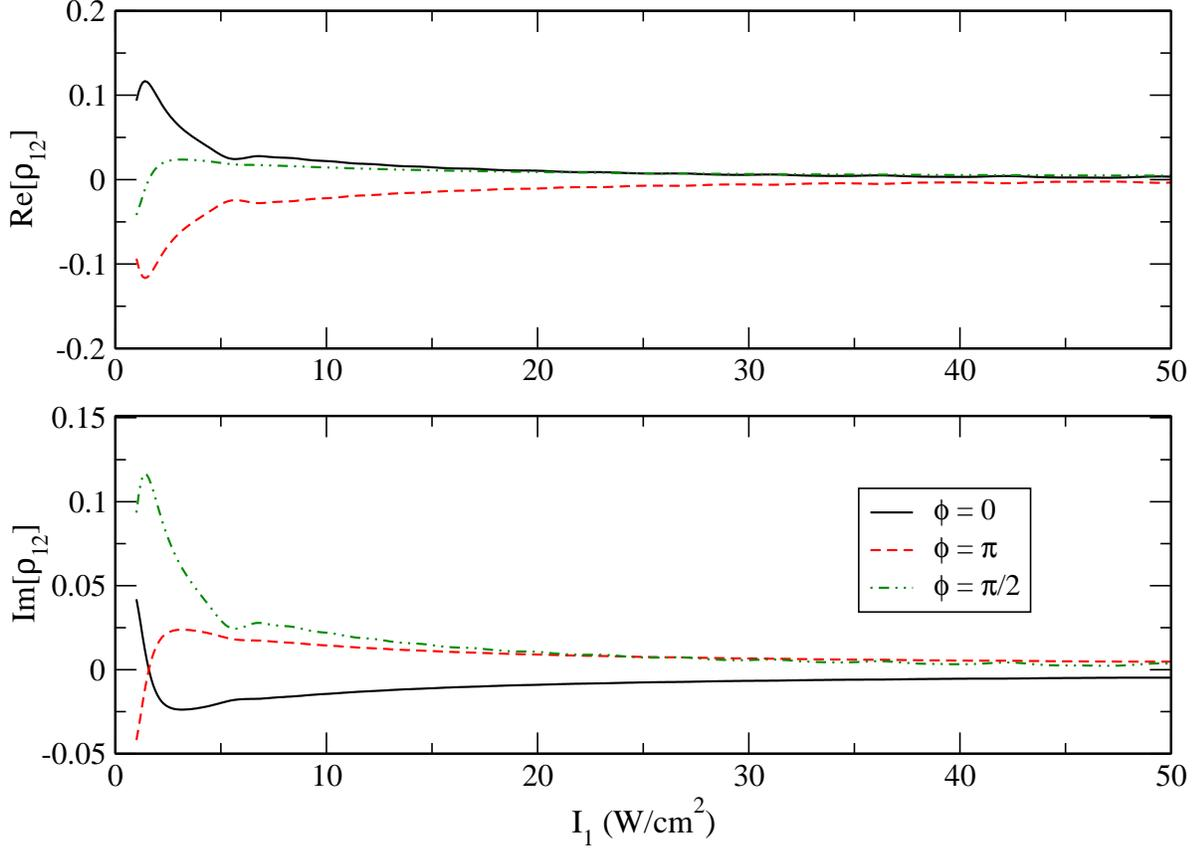


Figure 4. (Color online) $\text{Re}[\rho_{12}(0)]$ and $\text{Im}[\rho_{12}(0)]$ are plotted against I_1 (in unit of W cm^{-2}) for different values ϕ of the difference between the phases of the two lasers in upper and lower panels, respectively. The other parameters are $I_2 = 1 \text{ W cm}^{-2}$ and $\delta_1 = \delta_2 = 0$

where

$$\hat{\Sigma}_{\kappa\sigma}^+(t) = \sum_{n=1}^2 e^{-i\omega_{Ln}t} \int dE \hat{S}_{0E}^\dagger e^{i(\omega_E - \omega_{b_0})t} A_{nE}^* V_{n0}(\kappa\sigma) \quad (21)$$

Tracing over the vacuum states, we obtain

$$\begin{aligned} \frac{\partial}{\partial t} \{\rho_S^I(t)\} = & - \sum_{\kappa,\sigma} \int_0^t d\tau \left\{ e^{-i\omega_\kappa\tau} \left[\hat{\Sigma}_{\kappa\sigma}^+(t), \hat{\Sigma}_{\kappa\sigma}^-(t-\tau) \rho_S^I(t-\tau) \right] \right. \\ & \left. + \left[\hat{\Sigma}_{\kappa\sigma}^-(t), \hat{\Sigma}_{\kappa\sigma}^+(t-\tau) \rho_S^I(t-\tau) \right] \right\} + \text{H.c.} \quad (22) \end{aligned}$$

From equation (22), making use of Markoff approximation, we derive the equations of motion of reduced density matrix elements in dressed basis. These are

$$\dot{\rho}_{00} = \int dE \int dE' [\mathcal{A}_{EE'} \rho_{EE'} + \text{C.c}] \quad (23)$$

$$\dot{\rho}_{E0} = -i\omega_{E0} \rho_{E0} - \int dE' \mathcal{A}_{E'E} \rho_{E'0} - \int dE' \mathcal{A}_{E'E'} \rho_{E0} \quad (24)$$

$$\dot{\rho}_{EE'} = -i\delta_{EE'} \rho_{EE'} - \int dE'' \mathcal{A}_{E''E} \rho_{E''E'} - \int dE'' \mathcal{A}_{E'E''} \rho_{EE''} \quad (25)$$

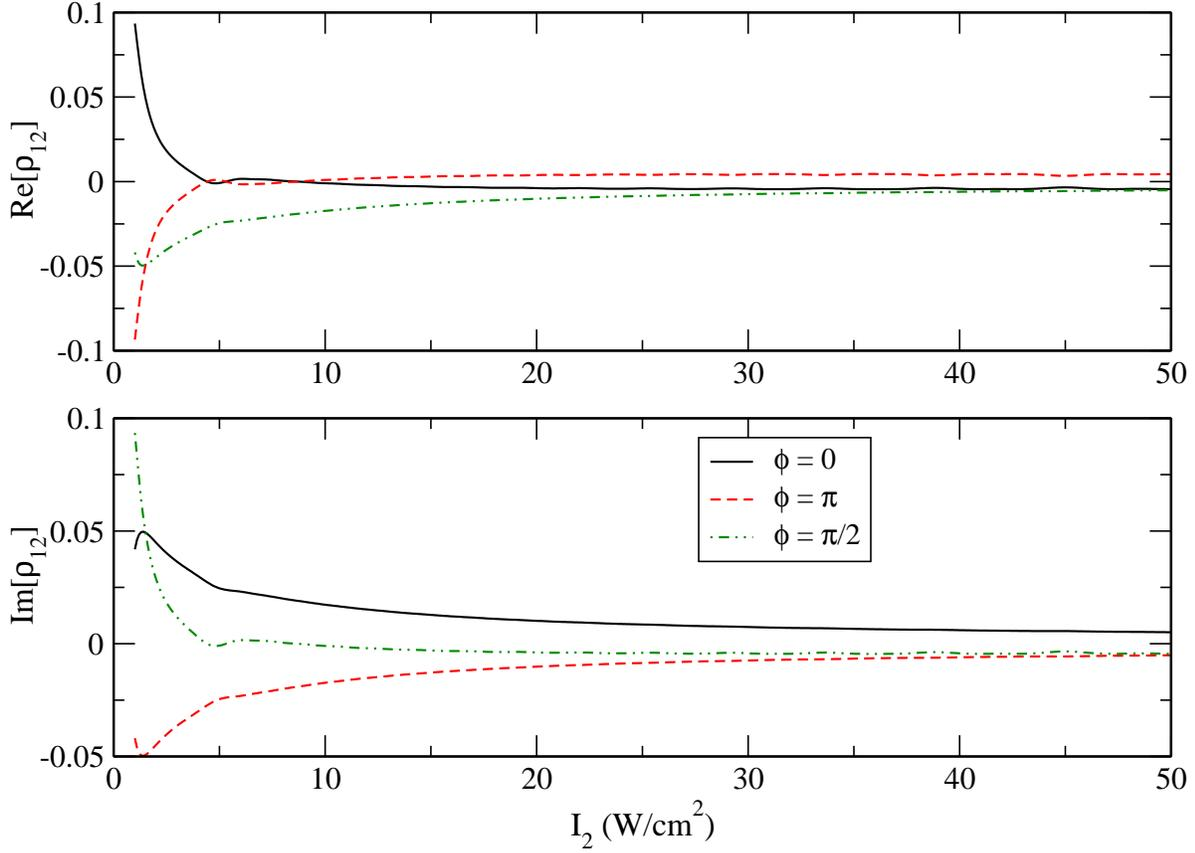


Figure 5. (Color online) Same as in figure 4, but as a function of I_2 keeping $I_1 = 1 \text{ W cm}^{-2}$

where $\delta_{EE'} = (E - E')/\hbar$ and

$$\mathcal{A}_{EE'} \simeq \frac{1}{2} \sum_{nn'} \gamma_{nn'} (\omega_n - \omega_{b_0}) \exp[i\delta_{nn'}t] A_{nE} A_{n'E'}^* \quad (26)$$

with $\delta_{nn'} = \omega_{L_n} - \omega_{L_{n'}}$ being the difference between n -th and n' -th lasers and

$$\gamma_{nn'} (\omega_n - \omega_{b_0}) \simeq \frac{\vec{D}_{n0} \vec{D}_{0n'} (\omega_n - \omega_{b_0})^3}{3\pi\epsilon_0 c^3 \hbar} \quad (27)$$

$\gamma_{nn'}(x)$ is a function of x . γ_{nn} is the spontaneous linewidth of n th excited state and $\gamma_{12} = \gamma_{21}$ is the vacuum-induced coupling between the two excited states [12, 13]. Note that in Eq. (27) we have neglected the light shift of the excited levels in comparison to the transition frequency $\omega_{n0} = \omega_n - \omega_{b_0}$ which is in the optical frequency domain while the typical light shifts as shown in Fig.3 are of the order of MHz. The expression (27) is obtained in the following way: We first substitute equation (21) into equation (22) and express the vacuum coupling V_{n0} in terms of corresponding bound-bound transition dipole moment \vec{D}_{n0} as described after equation (3). The sum over κ and σ is replaced by an integral over the infinite vacuum modes. Using standard Markoffian approximation, one can carry out first the integration over τ and then over the vacuum modes to arrive at the expression for $\gamma_{nn'}$ as given in equation (27). The normalization condition is

$$\rho_{00} + \int \rho_{EE} dE = 1 \quad (28)$$

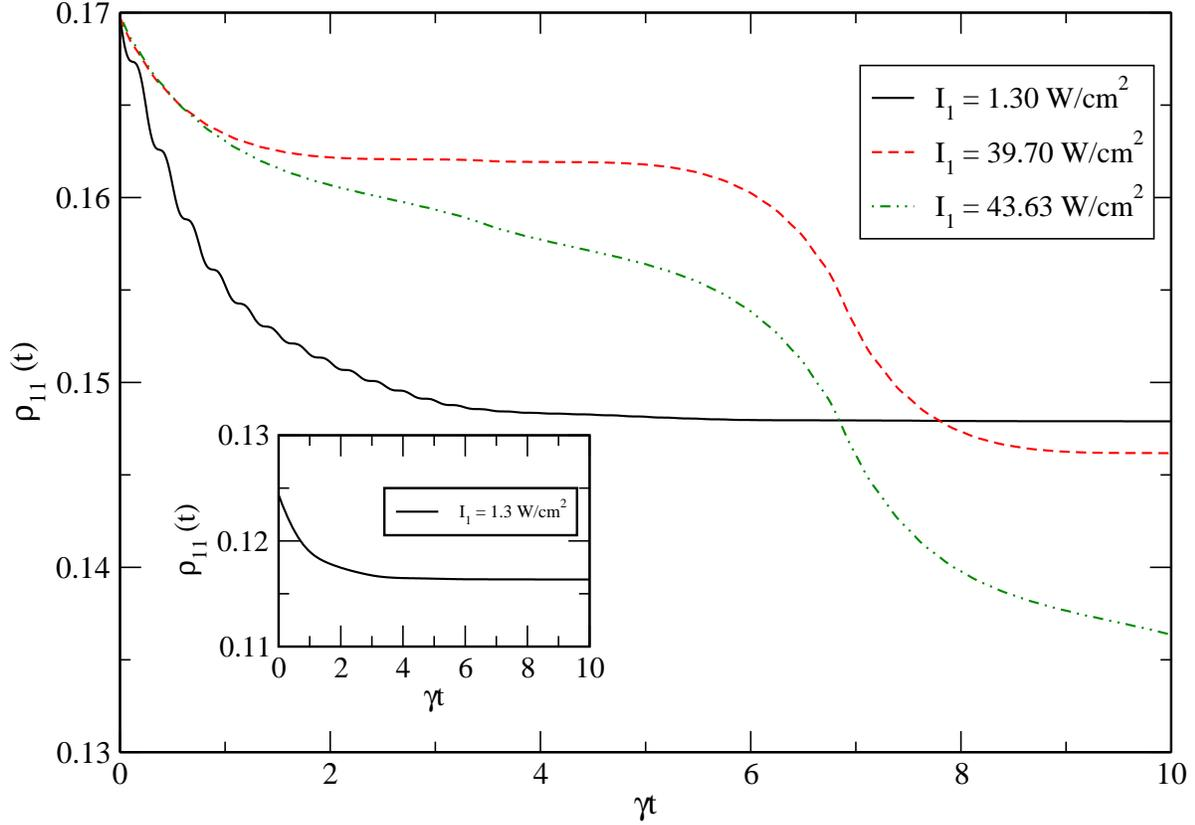


Figure 6. (Color online) ρ_{11} as a function of dimensionless unit γt for different values I_1 for $I_2 = 1 \text{ W cm}^{-2}$, $\delta_1 = \delta_2 = 0$ and $\phi = 0$. The inset shows the plot of ρ_{11} when laser-2 is switched off and $I_1 = 1.3 \text{ W cm}^{-2}$, $\delta_1 = 0$ and $\theta_1 = 0$.

Equations (23)-(25) form a set of three integro-differential equations for the density matrix elements expressed in the dressed continuum basis.

4. Solution

The density matrix elements can be expressed in bare basis by the transformation

$$\rho_{nn'} = \int dE \int dE' A_{nE} A_{n'E'}^* dE' \rho_{EE'} \quad (29)$$

In interaction picture, $\rho_{EE'}^I = \exp(i\delta_{EE'}t)\rho_{EE'}$ and the equation (25) can be rewritten as

$$\dot{\rho}_{EE'}^I = - \int dE'' \mathcal{A}_{E''E} \rho_{E''E'}^I e^{i\delta_{EE''}t} - \int dE'' \mathcal{A}_{E'E''} \rho_{EE''}^I e^{i\delta_{E''E'}t}. \quad (30)$$

The solution of the above equation can be formally expressed as

$$\begin{aligned} \rho_{EE'}^I(t) = & \delta(E - E') - \int_0^t dt' \int dE'' \mathcal{A}_{E''E}(t') e^{i\delta_{EE''}t'} \rho_{E''E'}^I(t') \\ & - \int_0^t dt' \int dE'' \mathcal{A}_{E'E''}(t') \rho_{EE''}^I(t') e^{i\delta_{E''E'}t'} \end{aligned} \quad (31)$$

The delta function on the right hand side is the initial value $\rho_{EE'}^I(0)$. The quantity $A_{EE'}(t)$ given in equation. (26) is expressed in terms of the product $A_{nE} A_{n'E}^*$ of the amplitudes of

the n th and n' th bound states in energy-normalized dressed continuum of equation (4). If vacuum couplings are neglected, the bound-state probability densities are given by $\rho_{nn} = \int dE |A_{nE}|^2 dE$ and the coherence terms $\rho_{nn'} = \int dE A_{nE} A_{n'E}^*$ with $n' \neq n$. It is important to note that, apart from causing spontaneous decay of the n th bound-state probability with decay constant γ_{nn} , vacuum couplings of the two excited bound states $|b_1\rangle$ and $|b_2\rangle$ with the ground bound-state $|b_0\rangle$ effectively give rise to vacuum-induced coherence (VIC) [19] between the two excited bound states with coupling constant γ_{12} . Recently, atom-molecule coupled photoassociative systems are shown to be better suited for realizing VIC [13]. Though the quantities $\gamma_{nn'}$ are calculable from equation (27) when the molecular transition dipole moments D_{n0} are given, for simplicity of our model calculations, we have set $\gamma_{11} = \gamma_{22} = \gamma_{12} = \gamma_{21} = \gamma$. In fact, since we consider that both the excited bound states belong to the same vibrational level but differing only in rotational quantum number, the spontaneous linewidths γ_{11} and γ_{22} would not differ much. Furthermore, since $\gamma_{12} = \gamma_{21} \simeq \sqrt{\gamma_{11}\gamma_{22}}$, we have $\gamma_{12} = \gamma_{21} = \gamma$ for the case considered here. The stimulated line width $\Gamma_n(E)$ is a function of the collision energy E for the ground state scattering between the two ground state atoms. Both in the limits $E \rightarrow 0$ and $E \rightarrow \infty$, Γ_n vanishes. Let us fix an energy \bar{E} near which both $\Gamma_1(\bar{E})$ and $\Gamma_2(\bar{E})$ attain their maximum values. It is then possible to write equation (26) in the form

$$\mathcal{A}_{EE'}(t) = \frac{1}{\hbar} \sum_{nn'} \bar{\gamma}_{nn'} \exp[i\delta_{nn'}t] \bar{A}_{nE} \bar{A}_{n'E'}^* \quad (32)$$

where $\bar{\gamma}_{nn'} = \gamma / \sqrt{\Gamma_n(\bar{E})\Gamma_{n'}(\bar{E})}$ and $\bar{A}_{nE} = A_{nE} \sqrt{\hbar\Gamma_n(\bar{E})/2}$ are the dimensionless quantities. The absolute value of \bar{A}_{nE} is less than unity. Supposes, the intensities of the two lasers are high enough so that $\Gamma_n(\bar{E}) \gg \gamma$ for both the excited bound states. In that case, using $\bar{\gamma}_{nn'}$ or the product $\bar{\gamma}_{nn'} \bar{A}_{nE} \bar{A}_{n'E'}^*$ as a small parameter, we can expand equation (30) in a time-ordered series

$$\begin{aligned} \rho_{EE'}^I(t) &= \delta(E - E') - \int_0^t dt' \mathcal{A}_{E'E}(t') e^{i\delta_{EE'}t'} - \int_0^t dt' \mathcal{A}_{E'E}(t') e^{i\delta_{EE'}t'} \\ &+ \int_0^t dt' \int dE'' \mathcal{A}_{E''E}(t') e^{i\delta_{EE''}t'} \times \int_0^{t'} dt'' \mathcal{A}_{E'E''}(t'') e^{i\delta_{E''E'}t''} \\ &+ \int_0^t dt' \int dE'' \mathcal{A}_{E''E}(t') e^{i\delta_{EE''}t'} \int_0^{t'} dt'' \mathcal{A}_{E'E''}(t'') e^{i\delta_{E''E'}t''} \\ &+ \int_0^t dt' \int dE'' \mathcal{A}_{E'E''}(t') e^{i\delta_{E''E'}t'} \int_0^{t'} dt'' \mathcal{A}_{E''E}(t'') e^{i\delta_{EE''}t''} \\ &+ \int_0^t dt' \int dE'' \mathcal{A}_{E'E''}(t') e^{i\delta_{E''E'}t'} \int_0^{t'} dt'' \mathcal{A}_{E''E}(t'') e^{i\delta_{EE''}t''} + \dots \quad (33) \end{aligned}$$

It is worthwhile to point out that this method of solution is similar in spirit to that of time-dependent perturbation, however it differs in essence because we have used dressed state amplitude as a small parameter and not the atom-field coupling. If a large number of terms are taken, then the expansion essentially provides solution for any time. However, numerically calculating higher order terms becomes increasingly involved because of larger number of multiple integrals in energy variable appearing in higher order terms. We therefore restrict

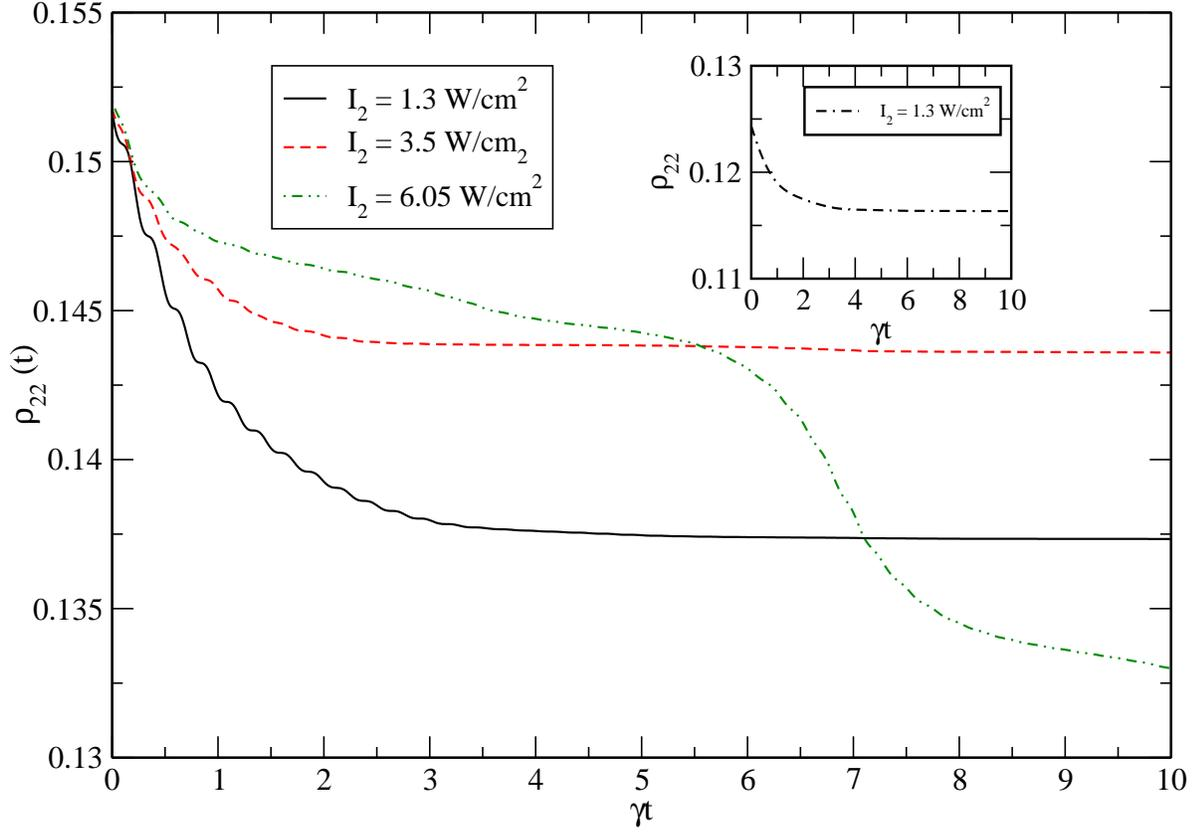


Figure 7. (Color online) $\rho_{22}(t)$ is plotted as a function of γt for different values of I_2 for $I_1 = 1 \text{ W cm}^{-2}$, $\delta_1 = \delta_2 = 0$ and $\phi = 0$. The inset shows the plot of ρ_{22} when only laser-2 is switched on at intensity $I_2 = 1.3 \text{ W cm}^{-2}$, $\delta_2 = 0$ and $\theta_2 = 0$.

our numerical studies to a few leading order terms as described in the next section.

5. Results and discussions

Driven by the two strong lasers, the system is prepared in a dressed continuum given by equation (4). Since this state is an admixture of the two excited bound states, it is subjected to spontaneous emission. We include spontaneous emission by considering the dressed levels to decay to a third bound level, thereby neglecting the decay of the excited states to the ground-state continuum inside the dressed-state manifold.

To discuss the effects of the phase-difference $\phi = \theta_1 - \theta_2$ between the two lasers, the laser intensities I_1 and I_2 , and the detunings δ_1 and δ_2 on decay dynamics, we first rewrite the dressed-state amplitude $A_{nE}^{\ell m_\ell}$ of equation (5) in the form

$$A_{nE}^{\ell m_\ell} = e^{i\theta_n} \frac{\Lambda_{J_n M_n}^{\ell m_\ell}(E) + \mathcal{A}_{nn'}^{\ell m_\ell} e^{-i(\theta_n - \theta_{n'})}}{\mathcal{E}_n + i\mathcal{G}_n/2} \quad (34)$$

where $\mathcal{A}_{nn'}^{\ell m_\ell} = \xi_{n'}^{-1} \mathcal{K}_{nn'}^{\text{LL}}$ and

$$\mathcal{E}_n = E + \hbar\delta_n - (E_n + E_n^{\text{shift}} + E_{nn'}^{\text{shift}}), \quad n' \neq n. \quad (35)$$

The additional shift for the n th excited bound state due to laser-induced cross coupling with the other (n') excited bound state is

$$E_{nn'}^{\text{shift}} = \text{Re}[\xi_{n'}^{-1} \mathcal{K}_{nn'}^{\text{LL}} \mathcal{K}_{n'n}^{\text{LL}}] \quad (36)$$

Here $\mathcal{G}_n = \Gamma_n + \Gamma_{nn'}$ with $\Gamma_{nn'} = -2\text{Im}[\text{Re}[\xi_{n'}^{-1} \mathcal{K}_{nn'}^{\text{LL}} \mathcal{K}_{n'n}^{\text{LL}}]]$ being the contribution to the total stimulated line width due to the cross coupling. In expression (34), the first term in the numerator corresponds to single-photon transition amplitude due to n th laser while the second term describe a net 3-photon transition amplitude with 2 photons coming from the n' th laser and the other one from n th laser.

The foregoing discussion has so far remained quite general. Now, we apply our method to ultracold ^{174}Yb atoms. For numerical illustration, we use realistic parameters following the recent experimental [20, 21, 22, 23] and theoretical [24] works on PA with ^{174}Yb . We have chosen ^{174}Yb system because this offers some advantages compared to other systems. For instance, it has no hyperfine structure and the ground-state molecular potential of $^{174}\text{Yb}_2$ is spin-singlet only. Furthermore, it has spin-forbidden inter-combination transitions. The total rotational quantum number is given by $\vec{J} = \vec{J}_e + \vec{\ell}$ where J_e is the total electronic angular momentum. For numerical work, we specifically consider a pair of ^{174}Yb atoms being acted upon by two co-propagating linearly polarized cw PA lasers. The polarizations of both lasers are assumed to be same. This geometry is the same as used in Ref [18] for manipulation of d -wave atom-atom interactions. For our numerical work, we consider that the two lasers drive transitions to the molecular bound states 1 and 2 characterized by by the rotational quantum numbers $J_1 = 1$ and $J_2 = 3$, respectively; of the same vibrational level $v = 106$. The two bound states belong to 0_u^+ (Hund's case c) molecular symmetry meaning that the projection of J_e on the internuclear axis being zero. Since ^{174}Yb atoms are bosons, only even partial waves are allowed for the scattering between the two ground state atoms. Free-bound dipole transition selection rules then dictate that the bound state 1 can be accessed from s - and d -wave scattering states, while the bound state 2 is accessible from d - and g -wave only. Thus d -wave ground scattering state is coupled to both the excited states by the two PA lasers resulting in the laser-induced coupling term $\mathcal{K}_{nn}^{\text{LL}}$. In general, d -wave scattering amplitude is small at low energy. But, fortunately for ^{174}Yb atoms, there is a d -wave shape resonance [20, 21] in the μK temperature regime leading to significant enhancement in d -wave scattering amplitude at relatively short separations where PA transitions are possible. In our calculations we neglect g -wave contributions.

As we prepare the system in a desired dressed continuum, the populations of the two excited bound states and the coherence between them depend on the relative intensity and phase between the two lasers. In the absence of spontaneous emission (idealized situation), the dressed state properties correspond to the initial conditions for our model. figure 1 shows variation of the initial populations and the coherence as a function of the intensity of either laser for the intensity of the other laser being fixed at 1 W cm^{-2} . For all our numerical work, we set the spontaneous line width $\gamma = 2.29 \text{ MHz}$ [22].

The variation of stimulated line widths and light shifts of the two bound states of $^{174}\text{Yb}_2$ as a function of collision energy E for the laser intensities $I_1 = I_2 = 1 \text{ W cm}^{-2}$ and zero

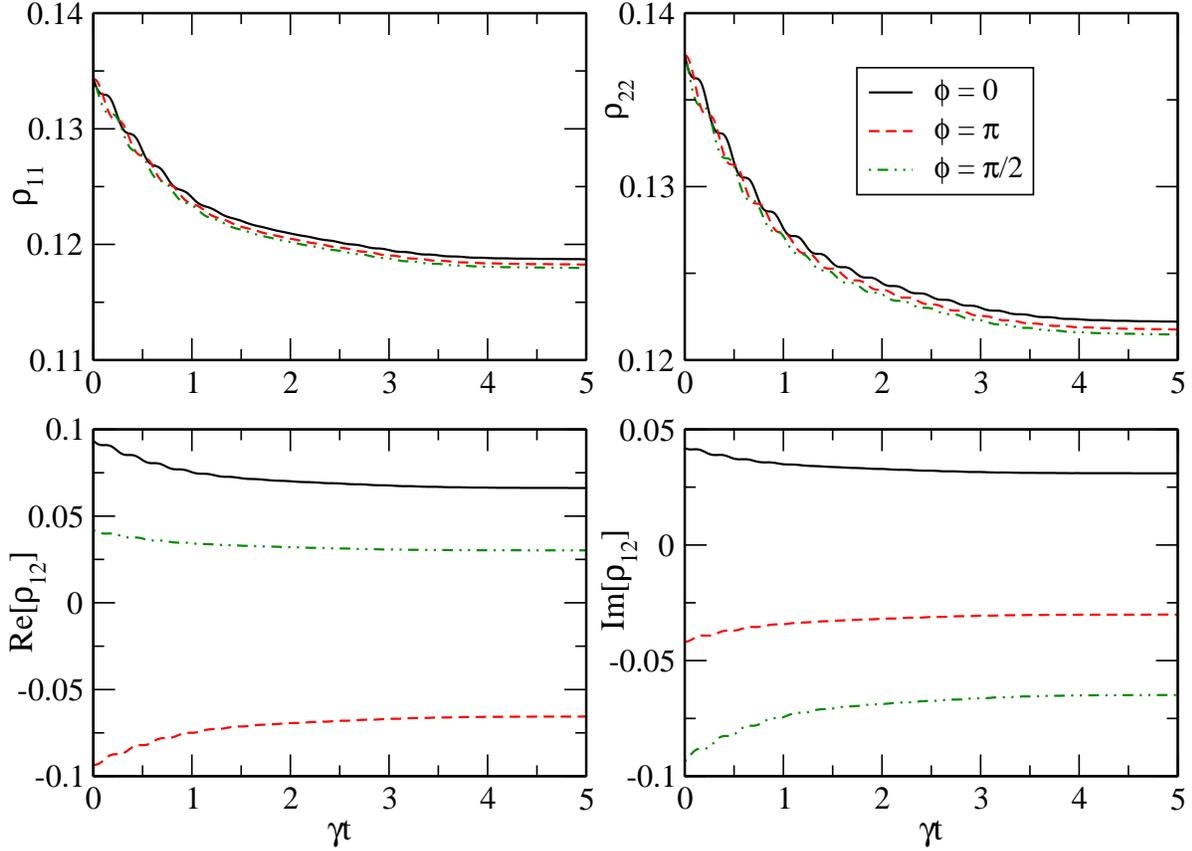


Figure 8. (Color online) $\rho_{nn'}(t)$ are plotted against γt for different values of ϕ but for fixed $I_1 = I_2 = 1 \text{ W cm}^{-2}$ and $\delta_1 = \delta_2 = 0$.

detunings are displayed in figure 2. The shift E_1^{shift} (stimulated line width Γ_1) is a sum of s - and d -wave partial shifts (stimulated line widths) while the shift E_2^{shift} and the stimulated line width Γ_2 are made of mainly d -wave partial shift and width, respectively; with no contribution from s -wave. From figure 2 we notice that the shifts of both bound states as a function of energy change rapidly from negative to positive value near $E = \bar{E} = 194 \mu\text{K}$ and the stimulated line widths of both bound states exhibit prominent peaks at that energy. This can be attributed to a d -wave shape resonance [20, 24]. We have found that the d -wave partial stimulated line widths of both the bound states near shape resonance are comparable. For the first bound state, the value of the d -wave partial stimulated line width near the resonance is found to exceed the s -wave partial line width by about 2 orders of magnitude. In figure 3, mutual light shift E_{12}^{shift} and stimulated line width Γ_{12} due to the coupling between the bound states are shown as a function of collision energy E in Hz. The mutual shifts and widths arise from the coupling of the d -wave scattering state with the two bound states by the two lasers. Owing to the existence of the d -wave shape resonance, the laser couplings of the d -wave scattering state to both bound states become significant, and so are the mutual shifts and stimulated line widths.

Figures 4 and 5 exhibit intensity-dependence of the coherence $\rho_{12}(0)$. The purpose of plotting these two figures is to assert that it is possible to prepare the dressed system

with a desirable coherence between the two excited bound states by judiciously selecting relative intensities and phases between the two lasers. It is interesting to note that d -wave shape resonance has a drastic effect on the properties of dressed continuum. Because of this resonance, the d -wave contributions to the amplitudes of transition to both the bound states are large even at a low temperature allowing an appreciable cross coupling to develop between the two bound states. For very large laser intensities at $\delta_1 = \delta_2 = 0$, light shifts would be so large that the system will be effectively far off resonant and therefore $\rho_{nn'}(0) \simeq 0$.

For calculating time-dependence of the density matrix elements for all the times, we need to calculate a large number of terms appearing on the right hand side of equation (33) order by order in $\bar{\gamma}_{nn'}$. This is a laborious and time-consuming exercise. Instead, to demonstrate the essential dynamical features arising from quantum superposition of the two rotational states, we restrict our study of decay dynamics to relatively short times. Inserting equation (26) in equation (33), retaining the terms up to first order in $\bar{\gamma}_{nn'}$, we have

$$\begin{aligned} \rho_{nn}(t) = & \tilde{A}_{nn}(0) - \gamma \int_0^t dt' \left[|\tilde{A}_{12}(t')|^2 + |\tilde{B}_{12}(t')|^2 + |\tilde{A}_{nn}(t')|^2 + |\tilde{B}_{nn}(t')|^2 \right] \\ & - 2\gamma \int_0^t dt' \text{Re} \left\{ \tilde{A}_{12}(t') \tilde{A}_{nn}(t') + \tilde{B}_{nn}(t') \tilde{B}_{12}(t') \right\} \cos(\delta_{12}t') + \dots \quad (37) \end{aligned}$$

where $\tilde{A}_{nn'}(t) = \int dE A_{nE}^* A_{n'E} \cos(\omega_E t)$ and $\tilde{B}_{nn'}(t) = \int dE A_{nE}^* A_{n'E} \sin(\omega_E t)$ with $\omega_E = E/\hbar$. Here $\tilde{A}_{nn}(0) = \int dE |A_{nE}|^2 = \rho_{nn}(0)$. Similarly, the coherence term ρ_{12} can be calculated up to the first order in $\bar{\gamma}_{nn'}$. These solutions hold good for $\gamma t < |\tilde{A}_{nn}(0)|^{-2}$ or equivalently, $\gamma t < |\rho_{nn}(0)|^{-2}$ for both $n = 1, 2$.

The decay dynamics of the populations $\rho_{11}(t)$ and $\rho_{22}(t)$ as a function of the scaled time γt are shown in figures 6 and 7, respectively. These results clearly exhibit that, when the system is strongly driven by two lasers, the decay is non-exponential and has small oscillations. The oscillations are particularly prominent for short times. In the long time limit the oscillations slowly die down. However, the oscillations can persist for long times if couplings are stronger. We have chosen the values of the laser intensities I_1 and I_2 such that the initial values of dressed population $\rho_{11}(t=0)$ or $\rho_{22}(t=0)$ are the same for those intensities. We notice that, though the values $\rho_{11}(0)$ (or $\rho_{22}(0)$) for a set of I_1 values for a fixed I_2 value (or a set of I_2 values for a fixed I_1) are the same, their time evolution is quite different and strongly influenced with the relative intensity of the two lasers. That the population oscillations result from the laser-induced coherence between the two bound states can be inferred by observing the decay of the populations when either of the lasers is switched off. Plots of ρ_{11} and ρ_{22} against γt for only laser-1 and laser-2 switched on, respectively are illustrated in the insets of figures 6 and 7 which show exponential decay of the populations $\rho_{11}(t)$ and $\rho_{22}(t)$ with no oscillations. When only one laser is tuned near the resonance of either bound state, we do not have any coherence between the two bound states. As the two excited bound states are about 57 MHz apart, one of the bound states remains far off-resonant in case of single-laser driving. As a result, the decay of the driven bound state occurs independent of the other bound state. The laser-induced coherence between the two bound states is developed only when we apply both the lasers.

The dynamical characteristics of population decay can be interpreted by analyzing the

time-dependence and relative contributions of the two expressions within the third and second brackets on the RHS of equation (37). Since $\delta_{12} \simeq -57$ MHz and the free-bound couplings are most significant near $E \simeq \bar{E} \sim 4$ MHz as can be noticed from figure 2, we may perform the time integration on the terms associated with $\cos(\delta_{12}t)$ in equation (37) in the slowly varying envelope approximation to obtain

$$-2\gamma \text{Re} \left\{ \tilde{A}_{12}(t)\tilde{A}_{nn}(t) + \tilde{B}_{nn}(t)\tilde{B}_{12}(t) \right\} \sin(\delta_{12}t)/\delta_{12} \quad (38)$$

Further, since in energy integrations the major contributions will come from energies near $E \simeq \bar{E}$, we may approximate

$$\tilde{A}_{nn'}(t) = \int dE A_{nE}^* A_{n'E} \cos(\omega_E t) \simeq \cos(\omega_{\bar{E}} t) \rho_{nn'}(0) \quad (39)$$

Similarly, $\tilde{B}_{nn'} \simeq \sin(\omega_{\bar{E}} t) \rho_{nn'}(0)$. Using these approximations, we get

$$\begin{aligned} \rho_{nn}(t) \sim & \rho_{nn}(0) - \gamma t [|\rho_{12}(0)|^2 + \rho_{nn}(0)^2] \\ & - 2\gamma \text{Re} \{ \rho_{12}(0) \rho_{nn}(0) \} \sin(\delta_{12}t)/\delta_{12} + \dots \end{aligned} \quad (40)$$

This expression clearly shows that when the quantities $(|\rho_{12}(0)|^2 + \rho_{nn}(0)^2)$ and $2\text{Re}(\rho_{12}(0)\rho_{nn}(0))$ are of comparable magnitude, we expect oscillations in population decay with time period $\tau_{\text{osc}} \simeq 2\pi/|\delta_{12}| \simeq 0.11$ in unit of γ^{-1} . When the laser intensities are not too high to induce large shifts, we would expect the qualitative features of the oscillations will be largely governed by one time scale which is τ_{osc} . In fact, the solid black curves in figures 6 and 7 clearly demonstrate oscillatory modulations with time scale τ_{osc} . However, when the laser intensities are high enough so that the energy-dependent shifts and stimulated line widths are appreciable for a range of energies around $E = \bar{E}$, then expression (40) would not be useful to indicate correct qualitative features. In that case, we need to retain full time dependence which will introduce another time scale $2\pi/\omega_{\bar{E}}$ which is, in the present context, roughly equal to 2π in unit of γ^{-1} . In such situations the net result would be a competition between oscillations with the two time scales. The plots in figures 6 and 7 at larger laser intensity or intensities clearly demonstrate such oscillatory modulations of the population decay with two time scales. It is particularly important to note that for larger intensity and appropriate detunings, the early population decay can be made much slower for an appreciable time duration. It is worthwhile to point out that, this analysis is done only to gain insight into the physics of the decay dynamics of the system, all the results presented here are obtained by numerically integrating over time t' and the entire range of energy.

Figure 8 shows the effects of ϕ on the temporal evolution of the populations ρ_{nn} and the coherence terms $\rho_{nn'}$ with $n \neq n'$. Though ϕ does affect the behavior of the oscillations in population decay, the magnitude of the populations at a time t is not altered much with the change of ϕ . In contrast, the magnitudes of the real and imaginary parts of the coherence term ρ_{12} are largely influenced by ϕ . When ϕ is altered by π , the sign of both real and imaginary parts of ρ_{12} changes.

Finally, we discuss quantum beats by studying the temporal evolution of the intensity of light emitted from the two correlated excited bound states. Quantum beats are manifested as oscillations in the emitted radiation intensity I_{qb} as a function of time [11, 12], which is given

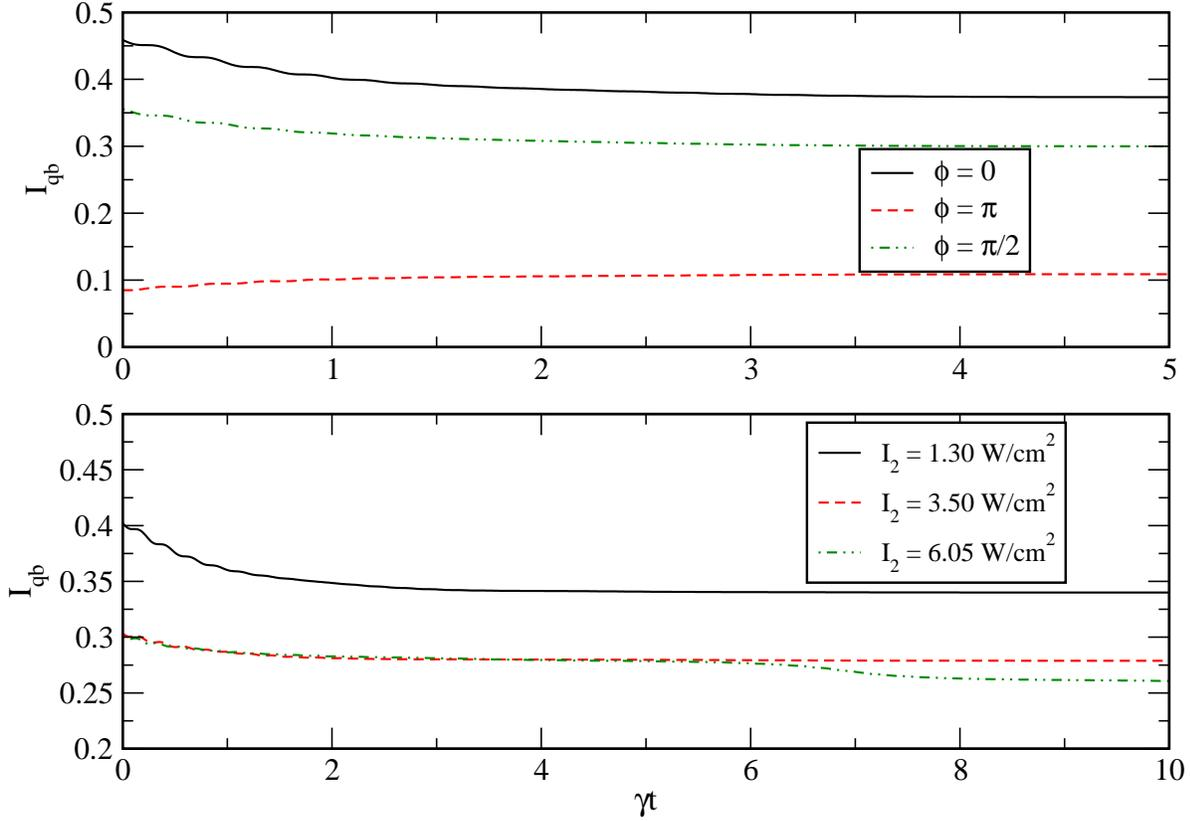


Figure 9. (Color online) In upper panel, we plot I_{qb} against γt for different values of ϕ when other parameters are fixed as $I_1 = I_2 = 1 \text{ W/cm}^2$ and $\delta_1 = \delta_2 = 0 \text{ MHz}$. In lower panel I_{qb} is plotted as a function of γt for different values of I_2 for $I_1 = 1 \text{ W/cm}^2$, $\phi = 0$ and $\delta_1 = \delta_2 = 0 \text{ MHz}$.

by

$$I_{qb}(t) = \gamma(\rho_{11}(t) + \rho_{22}(t) + 2\text{Re}[\rho_{12}(t)]) \quad (41)$$

In lower panel of figure 9 we show the effects of laser phase ϕ on quantum beats in time-dependent fluorescent intensity. The effects of different intensities of laser-2 on quantum beats are illustrated in the lower panel of same figure. We demonstrate the effects of different detunings on quantum beats in Fig. 10. Because of the mutual light shift E_{12}^{shift} between the two bound states due to coupling term $\mathcal{K}_{12}^{\text{LL}}$, the resonance conditions in case of two PA lasers are altered in comparison to those in single PA laser case. This leads to the non-monotonous effects of detunings on quantum beats as shown in figure 10.

Before ending this section, we wish to make a few remarks on the possibility of experimental demonstration of the physical effects discussed here. Our model can be easily realisable with currently available technology of high precision PA spectroscopy. Ultracold bosonic Yb or Sr atoms appear to be most suitable for this purpose. Because, they offer several advantages. First, their electronic ground state is purely singlet and has no hyperfine structure. This means that the bare continuum has no multiplet structure and so there is only one ground-state channel. Second, they have narrow line singlet-triplet inter-combination transitions. Third, they have long-range excited bound states which are accessible via PA

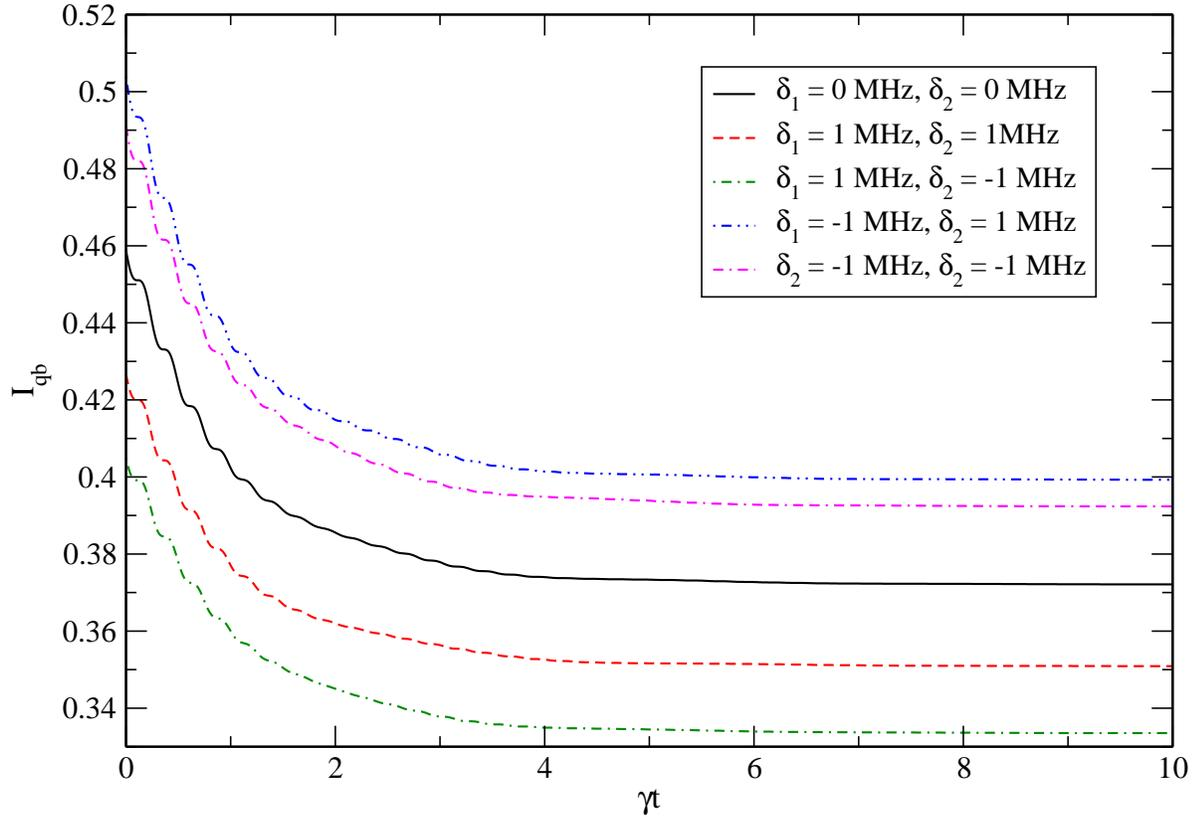


Figure 10. (Color online) I_{qb} is plotted against γt for different values of detuning parameters. Other parameters are fixed as $I_1 = I_2 = 1 \text{ W/cm}^2$ and $\phi = 0$.

[24]. These bound states have relatively long life time (\sim microsecond). It is possible to selectively drive two rotational levels as required for the model. Furthermore, since both the excited bound states have the same vibrational quantum number, their outer turning points will lie almost at the same separation. Because of long-range nature of these excited bound states that are strongly driven by the two lasers from the bare continuum, these two excited bound states are expected to have the largest Franck-Condon overlap with the near-zero energy or the last bound state in the ground electronic potential. It is therefore quite natural that these two driven bound states will predominantly spontaneously decay to the last bound state. In fact, the scattering length of Yb atoms have been experimentally determined by detecting the last bound state via two-colour PA spectroscopy [23], since the energy of the last bound state and the scattering length are closely related. All these facts indicate that our model is a realistic one and the predicted excited state coherence and the resulting quantum beats can be experimentally realisable.

6. Conclusions

In conclusion we have developed a theoretical treatment for the decay and decoherence from a pair of correlated excited molecular states in a strongly driven atom-molecule coupled system. We have shown that it is possible to create coherence between two excited molecular states

by strong-coupling photoassociation with two lasers. The transitions between these excited states may be electric dipole-forbidden. Our theoretical results have demonstrated that the spontaneous emissions from these two correlated excited bound states are strongly influenced by the coherence between them. In particular, the spontaneous emission has been shown to occur non-exponentially with multiple time scales due to the coherence. The linewidths and light shifts are shown to be largely affected by the coherence leading to the suppression of spontaneous emission and decoherence. Our results have revealed that the coherence can be detected as oscillations in decay and decoherence dynamics. We have further shown that the phase-difference between the two lasers can be used as a knob to change the phase of these oscillations. We have also demonstrated quantum beats in fluorescence light as a signature of the coherent superposition between the two excited states. We have discussed the possibility of experimental realization of our model.

Finally, our work may be useful in stimulating further studies on laser manipulation of the continuum and the bound states between ultracold atoms. Laser dressing of continuum-bound coupled systems in the context of autoionisation and photoionisation had been extensively studied earlier demonstrating many interesting effects such as “confluence of coherences” [25], population trapping with laser-induced continuum structure [26], non-decaying dressed-states in continuum [27], line-narrowing of autoionizing states [28], etc.. Our model can be extended to explore analogous effects in a new parameter regime at the photoassociative interface [29] of ultracold atoms and molecules.

Acknowledgment

AR is grateful to CSIR, Govt. of India, for a support.

References

- [1] Agarwal G S, Haan S L, Burnett K and Cooper J 1982 *Phys. Rev. Lett.* **48** 1164 (1982); Agarwal G S, Haan S L and Cooper J 1984 *Phys. Rev. A* **29** 2552
- [2] Lewenstein M, Haus J W, and Rzazewski K 1983 *Phys. Rev. Lett.* **50** 417; Haus J W, Lewenstein M, and Rzazewski K 1983 *Phys. Rev. A* **28** 2269
- [3] Agassi D, Rzazewski K, and Eberly J H 1983 *Phys. Rev. A* **28** 3648
- [4] Fano U 1961 *Phys. Rev.* **124** 1866
- [5] Breit G 1933 *Rev. Mod. Phys.* **5** 91
- [6] Corney A and Series G W 1964 *Proc. Phys. Soc.* **83** 213 ; Dodd J N, Kaul R D and Warrington D M 1964 *Proc. Phys. Soc. London* **84** 176
- [7] Hansch T W 1972 *Appl. Opt.* **11** 895; Gornik W *et al.* 1972 *Opt. Commun.* **6** 327
- [8] Haroche S, Paisner J A and Schawlow A L 1973 *Phys. Rev. Lett.* **30** 948
- [9] Hegerfeldt G C and Plenio M B 1993 *Phys. Rev. A* **47** 2186
- [10] Scully M O and Zubairy M S 1997 *Quantum Optics* (Cambridge, New York)
- [11] Zhou P and Swain S 1998 *J. Opt. Soc. Am. B* **15** 2593
- [12] Ficek Z and Swain S 2007 *Quantum Interference and Coherence* (Springer, New York).
- [13] Das S, Rakshit A and Deb B 2012 *Phys. Rev. A* **85** 011401(R) .
- [14] Rabi I I 1937 *Phys. Rev.* **51** 652.
- [15] Bloch F and Siegert A 1940 *Phys. Rev.* **57** 522.
- [16] Grifoni M and Hanggi P 1998 *Physics Reports* **304** 229354
- [17] Thimm B, Nalbach P and Terzidis O 1999 *Eur. Phys. J. B* **9** 207214
- [18] Deb B 2012 *Phys. Rev. A* **86** 063407

- [19] Agarwal G S 1974 *Springer Tracts in Modern Physics: Quantum Optics* (Springer-Verlag, Berlin)
- [20] Tojo S et al. 2006 *Phys. Rev. Lett.* **96**, 153201
- [21] Enomoto K, Kitagawa M, Kasa K, Tojo S, and Takahashi Y 2007 *Phys. Rev. Lett.* **98** 203201
- [22] Enomoto K, Kasa K, Kitagawa M, and Takahashi Y 2008 *Phys. Rev. Lett.* **101** 203201
- [23] Kitagawa M et al. 2008 *Phys. Rev. A* **77** 012719
- [24] Borkowski M et al. 2009 *Phys. Rev. A* **80** 012715
- [25] Rzazewski K and Eberly J H 1981 *Phys. Rev. Lett.* **47** 408
- [26] Coleman P E, Knight P L and Burnett K 1982 *Opt. Commun.* **42** 171; Coleman P E and Knight P L 1983 *J. Phys. B* **15** L235; Deng Z and J. H. Eberly J H 1984 *J. Opt. Soc. Am. B* **1** 102; Lami A and Rahman N K 1986 *Phys. Rev. A* **33** 782 ; Kyrola E 1986 *J. Phys. B.* **19** 1437
- [27] Haan S L and Agarwal G S 1987 *Phys. Rev. A* **35** 4592
- [28] Liu J L, McNicholl P, Harmin D A, Ivri J, Berfeman T and Metcalf H J 1985 *Phys. Rev. Lett.* **55**, 189 ; Feneuille S, Liberman S, Luc-Koenig E, Pincard J, and Taleb A 1985 *J. Phys. B* **15**, 1205
- [29] Deb B, Rakshit A, Hazra J and Chakraborty D 2013 *Pramana Journal of Physics* **80** 3